Published in final edited form as:
Mol Cell Biochem. 2004 ; 256-257(1-2): 281–289.

Mapping hypoxia-induced bioenergetic rearrangements and metabolic signaling by ^{18}O-assisted ^{31}P NMR and ^{1}H NMR spectroscopy

Darko Pucar[1], **Petras P. Dzeja**[1], **Peter Bast**[1], **Richard J. Gumina**[1], **Carmen Drahl**[1,2], **Lynette Lim**[1], **Nenad Juranic**[2], **Slobodan Macura**[2], and **Andre Terzic**[1]

[1] Division of Cardiovascular Diseases, Departments of Medicine, Molecular Pharmacology and Experimental Therapeutics, Rochester, MN, USA

[2] Biochemistry and Molecular Biology, Mayo Clinic, Mayo Foundation, Rochester, MN, USA

Abstract

Brief hypoxia or ischemia perturbs energy metabolism inducing paradoxically a stress-tolerant state, yet metabolic signals that trigger cytoprotection remain poorly understood. To evaluate bioenergetic rearrangements, control and hypoxic hearts were analyzed with ^{18}O-assisted ^{31}P NMR and ^{1}H NMR spectroscopy. The ^{18}O-induced isotope shift in the ^{31}P NMR spectrum of CrP, βADP and βATP was used to quantify phosphotransfer fluxes through creatine kinase and adenylate kinase. This analysis was supplemented with determination of energetically relevant metabolites in the phosphomonoester (PME) region of ^{31}P NMR spectra, and in both aromatic and aliphatic regions of ^{1}H NMR spectra. In control conditions, creatine kinase was the major phosphotransfer pathway processing high-energy phosphoryls between sites of ATP consumption and ATP production. In hypoxia, creatine kinase flux was dramatically reduced with a compensatory increase in adenylate kinase flux, which supported heart energetics by regenerating and transferring β- and γ-phosphoryls of ATP. Activation of adenylate kinase led to a build-up of AMP, IMP and adenosine, molecules involved in cardioprotective signaling. ^{31}P and ^{1}H NMR spectral analysis further revealed NADH and H^+ scavenging by α-glycerophosphate dehydrogenase (αGPDH) and lactate dehydrogenase contributing to maintained glycolysis under hypoxia. Hypoxia-induced accumulation of α-glycerophosphate and nucleoside 5′-monophosphates, through αGPDH and adenylate kinase reactions, respectively, was mapped within the increased PME signal in the ^{31}P NMR spectrum. Thus, ^{18}O-assisted ^{31}P NMR combined with ^{1}H NMR provide a powerful approach in capturing rearrangements in cardiac bioenergetics, and associated metabolic signaling that underlie the cardiac adaptive response to stress.

Keywords

adenylate kinase; creatine kinase; metabolism; heart; energetics; ischemia

Introduction

Oxygen deficiency associated with hypoxic or ischemic stress in heart muscle disrupts mitochondrial oxidative phosphorylation compromising ATP production and associated ATP-dependent cellular processes [1–6]. Yet, brief energetic insults alter intracellular metabolic and signal transduction triggering an adaptive protective response [7–13]. In particular, cellular

Address for offprints: A. Terzic, Guggenheim 7, Mayo Clinic, 200 First Street SW, Rochester, MN 55905, USA (E-mail: terzic.andre@mayo.edu).

phosphotransfer relays, catalyzed by creatine kinase (CK) and adenylate kinase (AK), have been implicated in the maintenance of nucleotide levels and transfer of high-energy phosphoryls between sites of ATP production and consumption [14–23]. The contribution of phosphotransfer enzymes in supporting heart metabolism under hypoxia has been inferred from changes in substrate levels and measurements of phosphoryl exchange rates [1,24–30]. More recently, the significance of individual phosphotransfer pathways following ischemia-reperfusion in ischemia-preconditioned and AK1-deficient myocardium was demonstrated by assessment of high-energy phosphoryl flux [11,22,32]. To gain further insight into metabolic signaling and cell tolerance to stress, it is essential to capture the dynamics of energy metabolism, and map adaptive phosphotransfer rearrangements along with originating metabolic signals.

In this regard, ^{18}O-assisted ^{31}P NMR spectroscopy was developed for simultaneous measurement of metabolite levels and metabolic fluxes through phosphotransfer systems [11,22,32–34]. Incorporation of ^{18}O as a result of cellular metabolic activity induces an isotope shift in the ^{31}P NMR spectrum of phosphoryl containing metabolites [35]. Although ^{18}O-induced isotope shift is rather small (around 0.025 ppm), it can be visualized and quantified using high-resolution NMR spectroscopy [11]. Originally, the ^{18}O induced isotope shift in the ^{31}P NMR spectrum was exploited to determine phosphotransfer reaction rates *in vitro* [35,36], and then adapted to monitor actual metabolic fluxes in intact heart muscle [11,22, 32]. Introduction of ^{18}O water in tissues of interest leads to ^{18}O incorporation into cellular phosphates according to the rate of involved phosphotransfer reactions (Fig. 1) [11,37–39]. Such property allows tracking of high-energy phosphoryl transfer routes, and quantification of respective enzymatic fluxes at different levels of cellular activity [11,19,22,32–34,37–40].

Here, combined ^{18}O-assisted ^{31}P NMR and ^{1}H NMR analysis demonstrated that the metabolic profile of the hypoxic heart is characterized by diminished creatine kinase flux and up-regulated adenylate kinase phosphotransfer, which supports myocardial energetics by regenerating and transferring β- and γ-phosphoryls of ATP. Activation of adenylate kinase flux, along with nucleotide hydrolysis, led to a build-up of AMP, IMP and adenosine, molecules involved in stress-adaptive signaling. The aromatic region of the ^{1}H NMR spectrum was particularly valuable for quantification of adenine nucleotides and their degradation products. Further, ^{31}P and ^{1}H NMR spectral analysis revealed that α-glycerophosphate dehydrogenase (αGPDH) has an important role in regulating glycolytic metabolism, and its product, α-glycerophosphate (αGP), significantly contributes to the phosphomonoester (PME) region in ^{31}P NMR spectra under hypoxia.

Materials and methods

Heart perfusion

Male Harlan Sprague Dawley guinea pigs (350–400 g) were heparinized (1000 U i.p.) and anesthetized (75 mg/kg ip pentobarbital). Excised hearts were perfused on a Langendorff appa-saturated Krebs-Henseleit (K-H) ratus with 95% O_2/5% CO_2 solution (in mmol/l: 123 NaCl, 6.0 KCl, 2.5 $CaCl_2$, 19 $NaHCO_3$, °C) 1.2 $MgSO_4$, 11.0 glucose, 0.5 EDTA, 20 U/L insulin, 37 at a perfusion pressure of 60 mmHg, and pacing rate at 250 beats/min.

Experimental protocols and ^{18}O-phosphoryl-labeling

'Control' hearts were perfused for 40 min with the K-H solution, and then switched for 30 sec to the K-H solution enriched with 40% ^{18}O water (Isotec) and freeze-clamped in liquid nitrogen. 'Hypoxic' hearts were perfused for 40 min with the K-H solution, then switched for 7 min to hypoxic K-H solution and finally switched for 30 sec to hypoxic K-H solution supplemented with 40% ^{18}O water, and freeze-clamped in liquid nitrogen. Hypoxic K-H

solution was produced by bubbling to reduce the oxygen partial pressure to with 95% N_2/5% CO_2 20–30 mmHg. As ^{18}O labeling displays an exponential kinetics with saturation occurring after 2 min [33], the 30 sec-long labeling performed here is within the initial linear phase of the ^{18}O labeling curve.

Nuclear magnetic resonance spectroscopy

To maximize resolution of ^{18}O induced shifts in ^{31}P NMR spectra and to increase sample stability, perchloric acid-extracted tissue were subjected to extensive chelation to remove divalent cations [11,22]. First, hearts were extracted in a solution containing 0.6 M perchloric acid and 1 mM EDTA. Proteins were pelleted by centrifugation (15,000 g, 10 min) and protein content determined with a D_C Protein Assay kit (Bio-Rad). Supernatants were neutralized with 2 M $KHCO_3$, pre-cleaned with the Chelex 100 resin (Sigma) at 4°C for 1 h, and supplemented with internal standards for ^{31}P and ^{1}H NMR, 375 nmol of methylene diphosphonate (MDP) and 50 nmol of 3-trimethylsilyl tetradeutero sodium propionate (TSP), respectively. Samples were then concentrated by vacuum-centrifugation (Savant) to a volume of 0.3 ml, filtered (centrifuge filter: 0.22 μm, Milipore), supplemented with 0.3 ml D_2O (Isotec), and chelated at 4°C for 12 h. Upon chelation, samples were frozen together with the Chelex resin in plastic ependorfs, with resin removed by filtration immediately before data acquisition.

^{31}P NMR and ^{1}H NMR data acquisition were performed at 202.5 and 500 MHz using a Bruker 11 T (Avance) spectrometer in high-quality 5 mm tubes (535-PP-7 Wilmad Glass) at ambient temperature and sample spinning at 20 Hz. Magnetic field homogeneity was maximized by 3D gradient shimming to achieve typical line width at a half height of 0.0012 ppm (0.6 Hz on 500 MHz) in a single ^{1}H NMR scan. During data acquisition auto-shimming (z1 and z2) was applied to maintain field homogeneity. Typical line widths at half height of various cellular phosphates in ^{31}P NMR spectra were around 0.0080 ppm (1.5 Hz on 202.5 MHz), significantly less then the ^{18}O-induced shift ranging between 0.0210 and 0.0250 ppm.

For ^{31}P NMR, 9000 scans were acquired without relaxation delay (acquisition time 1.61 sec) using a pulse width of 10 μsec (53° angle) with proton decoupling during data acquisition (WALTZ-16 with 90° angle, pulse width of 506 μsec for ^{1}H). Before Fourier-transformation FIDs were zero-filled to 32 K, and multiplied by an exponential window function with 0.3 Hz line-broadening. Peak areas were integrated using the Bruker software after automatic correction of phase and baseline. Deconvolution with the Nuts software (Acorn NMR) was applied where appropriate to determine areas of overlapping peaks. Chemical shifts were referenced according to CrP, which was set to be at −3.12 ppm relative to 85% orthophosphoric acid. ^{18}O labeling of metabolites were calculated as described below. The metabolite levels of glucoso-6-phosphate (G6P), α-glycerophosphate (αGP), inorganic phosphate (Pi), CrP, ATP, ADP were determined according to MDP used as an internal standard, and corrected for NOE (by factors determined in typical sample recorded with and without decoupling) and incomplete relaxation (by factors calculated from T_1 times in a typical sample, measured by the inversion-recovery technique) as described [11,22].

For ^{1}H NMR, 128 scans were accumulated under fully relaxed conditions (12.8 sec relaxation delay) with a pulse width of 9 μsec (90° angle). FIDs were zero-filled to 32 K, and Fourier-transformed without filtering. Phase and baseline were manually adjusted before integration and decon-volution. Chemical shifts were assigned relative to the TSP signal at 0 ppm. Metabolite levels of adenosine monophosphate (AMP), ATP, ADP, adenosine, inosine monophosphate (IMP), CrP and lactate (Lac) were calculated according to TSP used as internal standard. The identity of metabolites was confirmed by standard additions. After corrections, levels of CrP, ATP and ADP did not differ more then 10% between ^{31}P and ^{1}H NMR, and average values from these two alternative measurements were taken.

Calculation of phosphotransfer fluxes

Up to three ^{18}O atoms can be incorporated in phosphoryls of CrP, β-ADP and β-ATP. The percentages of ^{16}O, O_1,^{18} O_2^{18} and O_3^{18} phosphoryl species in CrP, β-ADP and β-ATP were proportional to integrals of their respective peaks in the ^{31}P MR spectrum [11,22,32]. Cumulative ^{18}O labeling was calculated as [%^{18} O_1+ 2(%^{18} O_2) + 3(%^{18} O_3)]/[3(%^{18}O in H_2O)] as previously described [11,19,37–40]. Creatine kinase phosphotransfer flux was determined from the rate of appearance of CrP species containing ^{18}O labeled phosphoryls using pseudo-linear approximation and assuming the creatine kinase reaction at steady-state [11,38,39]. Adenylate kinase phosphotransfer flux was determined from the rate of appearance of ^{18}O containing β-phosphoryls in ADP and ATP [19,22,32,40].

Statistical analysis

Data are expressed as mean ± S.E. Two-sided Student's *t*-test assuming unequal variances was used for statistical analysis. A difference at $p < 0.05$ was considered significant.

Results

Rearrangement in cellular phosphotransfer under hypoxia

In the well-oxygenated heart, transfer of high-energy phosphoryls between sites of ATP production and consumption is facilitated by the creatine kinase (CK) and adenylate kinase (AK) system, with creatine kinase phosphotransfer serving a dominant role [11,14–17,19,22, 29,32,41]. Here, with hypoxic challenge, CK phosphotransfer was dramatically reduced (Fig. 2). On average, CK flux dropped from 287 ± 4 nmol·mg protein^{-1}·min^{-1} under normoxia to 66 ± 18 nmol·mg protein^{-1}·min^{-1} in hypoxia ($p < 0.01$, $n = 5$ each), i.e. a 77% reduction (Fig. 3). Conversely, upon hypoxia, AK-catalyzed ^{18}O-labeling of β-phosphoryls of ADP and ATP was increased (Fig. 2). This translated in a 67% increase in AK flux, from 44 ± 2 nmol·mg protein^{-1}·min^{-1} in the normoxic to 73 ± 5 nmol·mg protein^{-1}·min^{-1} in the hypoxic myocardium ($p < 0.01$, $n = 5$ each; Figs 2 and 3). Reduction in the CK/AK flux ratio, from 6.5 ± 0.4 in normoxia to 0.8 ± 0.2 in hypoxia ($p < 0.01$, $n = 5$ each), indicates rearrangement in phosphotransfer signaling with adenylate kinase playing a major role in supporting heart energetics under hypoxic stress.

Biological significance of adenylate kinase activation

The imbalance between oxygen demand and supply under hypoxia resulted in a significant reduction of ATP and CrP levels (Fig. 2). On average, ATP dropped from 25.1 ± 1.0 nmol·mg protein^{-1} in normoxia to 14.0 ± 1.3 nmol·mg protein^{-1} in hypoxia ($p < 0.01$, $n = 5$ each, Figs 2 and 4A). Similarly, CrP was reduced from 36.8 ± 0.7 to 7.7 ± 1.2 nmol·mg protein^{-1} ($p < 0.01$, $n = 5$ each) under hypoxic conditions (Fig. 2). Consequently, in hypoxia, ADP increased from 4.9 ± 0.1 to 6.8 ± 0.3 nmol·mg protein^{-1} ($p < 0.01$, $n = 5$ each, Figs 2 and 4A), and inorganic phosphate increased from 27.8 ± 1.4 to 60.4 ± 2.6 nmol·mg protein^{-1} ($p < 0.01$, $n = 5$ each, Fig. 2). This resulted in a significant reduction, from 5.1 under control to 2.1 under hypoxic conditions, of the ATP/ADP ratio, an energetic signal balancing ATP production and consumption processes. Under hypoxia, activation of adenylate kinase phosphotransfer could increase regeneration of ATP by re-phosphorylating ADP through the ADP + ADP → ATP + AMP reaction, concomitantly producing AMP, an important signaling molecule. AMP and its degradation products, adenosine and IMP, were sharply increased under hypoxia, and detected with ^{1}H NMR (Fig. 4A). On average, AMP was 1.00 ± 0.12 and 2.41 ± 0.15 nmol·mg protein^{-1} ($p < 0.01$, $n = 5$ each groups), adenosine was 0.046 ± 0.003 and 0.254 ± 0.053 nmol·mg protein^{-1} ($p < 0.01$, $n = 5$ each), and IMP was 0.19 ± 0.06 and 1.47 ± 0.18 nmol·mg protein^{-1} ($p < 0.01$, $n = 5$ each) in normoxic and hypoxic hearts, respectively (Fig. 4B). Adenylate kinase activation also affected the appearance of the PME region in the ^{31}P spectrum

through increase of the nucleotide monophosphate (NMP) peak (Fig. 5). This NMP peak was composed of AMP, IMP, xantosine monophosphate (XMP), all confirmed by standard addition, and possibly by other monophosphates. Although due to a mixed composition the precise quantification of individual NMP components was not possible, such increase in the NMP peak can be used as an indicator of AK activation as it reflects production and further degradation of AMP, the main product of the AK reaction. Thus, adenylate kinase supports heart bioenergetics in hypoxia by maintaining ATP levels and inducing production of cardioprotective mediators, such as AMP, adenosine, and IMP, which activate downstream metabolic and signal transduction events [8–13,28,42–46].

Mapping by ^{31}P and ^{1}H NMR of altered glycolytic metabolism in hypoxia

In hypoxia, glycolysis is a major energetic system that could reduce the decline in ATP levels [1–4]. However, build-up of NADH and H^+ under hypoxic conditions can inhibit key glycolytic enzymes, phosphofructokinase (PFK) and glycer-aldehyde phosphate dehydrogenase (GAPDH) [1,3,25,47]. To prevent inhibition of glycolysis, NADH and H^+ must be scavenged. This could be accomplished by α-glycerophosphate dehydrogenase (αGPDH) and lactate dehydrogenase (LDH), resulting in increased α-glycerophosphate (α-GP) and lactate, detectable by ^{31}P and ^{1}H NMR, respectively [11]. Here, α-GP, a product of the αGPDH reaction, increased from 1.0 ± 0.2 nmol·mg protein^{-1} in normoxic to 13.7 ± 0.6 nmol·mg protein^{-1} in hypoxic hearts ($p < 0.01$, n = 5 each, Fig. 5). Also, lactate, a product of LDH catalysis and indicator of NADH scavenging, increased from 1.6 ± 0.4 nmol·mg protein^{-1} in normoxia to 17.9 ± 3.3 nmol·mg protein^{-1} in hypoxia ($p < 0.01$, n = 5 each). Similar increases in α-GP and lactate suggest that αGPDH and LDH contribute significantly to NADH and H^+ scavenging under hypoxia. Moreover, the increase in α-GP under hypoxic conditions leads to an in-creased PME region in ^{31}P NMR spectra (Fig. 5). The increase of α-GP was an order of magnitude higher compared to the 1.5 fold increase in glucose-6-phosphate (G6P) detectable in the same spectral area (Fig. 5). On average, G6P levels were 0.41 ± 0.02 and 0.64 ± 0.07 nmol·mg protein^{-1} ($p < 0.01$, n = 5 each) in normoxic and hypoxic hearts, respectively. Modest elevation in G6P, along with increase in α-GP and lactate levels in hypoxia, indicate a new steady-state in glycolytic metabolism without significant inhibition of PFK and/or GAPDH that would otherwise produce build-up of proximal glycolytic intermediates [47,48].

Discussion

Adaptive rearrangements in cellular energy metabolism have been implicated in the generation of a stress-tolerant state [7–15]. Here, ^{18}O-assisted ^{31}P NMR with ^{1}H NMR analysis mapped the bioenergetic dynamics of the myocardium under hypoxic stress. This comprehensive approach revealed a prominent role for adenylate kinase (AK) in supporting cardiac bioenergetics and metabolic signaling under hypoxic conditions. While in normoxia the majority of high-energy phosphoryl transfer proceeds through the creatine kinase (CK) system with a relatively minor contribution by AK [11,19,22,32], under hypoxia the rapid decline in CK-mediated phosphotransfer was associated with an apparently adaptive up-regulation of AK-catalyzed flux, and the generation of AMP, IMP and adenosine, molecules involved in cardioprotective signaling [8–13,42–46]. Moreover, ^{31}P and ^{1}H NMR spectral analysis revealed that scavenging of NADH and H^+, by α-glycerophosphate dehydrogenase (αGPDH) and lactate dehydrogenase (LDH), contributing to maintained glycolysis, which along with AK phosphotransfer supports cardiac bioenergetics under hypoxia.

Upon hypoxic stress, production of CrP in mitochondria is compromised due to unfavorable thermodynamic and kinetic conditions, leading to depletion of cytosolic CrP stores following regeneration of ATP through the CK-catalyzed reaction: CrP + ADP → ATP + Cr [16,24, 29]. Accordingly, CK-catalyzed phosphotransfer, measured here by ^{18}O-assisted ^{31}P NMR in

the direction of CrP production, was reduced 4-fold under hypoxic challenge. Concomitantly, AK-catalyzed ^{18}O-labeling of βADP and bATP was increased, resulting in essentially a doubling of AK flux. In addition to ^{18}O analysis that showed enhanced labeling of βADP and bATP, as a direct consequence of AK activation ^{31}P NMR spectra also demonstrated a sharp increase of the nucleoside monophosphate (NMP) signal in the region of phosphomonoester (PME) resonance. Components of the NMP signal (AMP, IMP and other nucleoside monophosphates) can be individually observed in the aromatic region (5–9 ppm) of ^{1}H spectra, along with other signals affected by AK, like adenosine. Increase in AMP and its degradation products, IMP and adenosine, provided further confirmation of AK activation.

Such activation of AK can protect heart muscle under hypoxia at various levels (Fig. 6). In particular, by regenerating ATP, providing a transfer mechanism for ATP between production and consumption sites, and ultimately by initiating AMP and adenosine production [11,19, 22,32]. Indeed, AK remains active in its ATP regenerating and transferring role as long as ADP is available and the enzyme is not inhibited by a build-up of AMP [49]. In fact, an increase in AMP is limited due to further AMP metabolism through AMP-deaminase and 5′ nucleotidase leading to production of IMP and adenosine, respectively [1,28,44]. Here, in hypoxic hearts, AMP levels were doubled, yet adenosine levels were increased essentially five times indicating high 5′ nucleotidase activity. Moreover, IMP levels were increased by more than 2 fold reflecting AMP degradation through the AMP-deaminase pathway in hypoxia. Thus, AK supports the bio-energetics of oxygen deficient hearts, in line with findings that hearts lacking AK1, the major cytosolic isoform of AK, display reduced ATP and adenosine levels, and an increased vulnerability to metabolic stress [22,32].

In addition, AK serves a distinct metabolic signaling role by translating small alterations in the ATP and ADP balance into large changes in AMP levels [18,49,51]. Indeed, AK phosphotransfer regulates nucleotide-dependent gating of ATP-sensitive potassium (K_{ATP}) channels [50–52], a membrane metabolic sensor implicated in stress adaptation and cardioprotection [53–55]. ^{18}O-assisted ^{31}P NMR analysis indicate a hypoxia-induced increase in AMP phosphorylation (ATP + AMP ↔ 2ADP), which would amplify metabolic signaling by providing 2 molecules of ADP for each ATP removed from ATP-sensitive cellular components [18,51]. Moreover, AMP produced in the reverse AK reaction can also activate metabolic sensors, such as AMP-dependent protein kinase [56,57] and glycolytic/ glycogenolytic enzymes [58], involved in stress adaptation and cellular protection. Besides AMP, other nucleotide degradation products such IMP, adenosine and inosine have distinct metabolic signaling roles, implicated in cardioprotection [28,42–46]. Thus, redistribution of flux between AK and CK phosphotransfer, observed under hypoxic challenge, contributes to reduction in bio-energetic deficit and initiation of signaling pathways implicated in cellular protection.

Alterations in glycolytic metabolism were also mapped using ^{31}P and ^{1}H NMR. Hypoxia induced marked increase in levels of α-GP and lactate, as a result of activation α-glycerophosphate dehydrogenase (αGPDH: dihydroxyacetone phosphate + NADH + H^+ → α-GP + NAD^+) and lactate de-hydrogenase (LDH: pyruvate + NADH + H^+ → lactate + NAD^+) responsible for scavenging NADH and H^+, critical suppressors of key glycolytic enzymes [1,3,25,47,58]. NADH accumulates under hypoxia since it can no longer be utilized for oxidative phosphorylation due to oxygen deficiency, while protons are produced during CrP and ATP breakdown [3,47,58]. Washout of lactate during hypoxic perfusion, in contrast to condition of no-flow ischemia, would maintain the LDH reaction supporting NADH scavenging [1,3,25,47]. That optimal scavenging did sustain glycolytic metabolism under hypoxia was further indicated by only modest increase in G6P, the glycolytic intermediate proximal to the GAPDH and PFK reactions. Larger elevations in G6P would have indicated

possible inhibition of GAPDH and PFK, and the inability of this intermediate to be processed through the glycolytic pathway [25,47,58].

The present use of high resolution ^{31}P NMR provided the opportunity to resolve components of the PME region in NMR spectra, which included G6P, α-GP, NMP and phospholipid compounds. This is of significance since increase in the PME peak area negatively correlates with functional performance of failing hearts and with recovery of heart muscle from metabolic challenge, such as ischemia [59–63]. Indeed, cardioprotective interventions are associated with reduction in the PME area [62,63], underscoring the importance of mapping individual components in the PME region with high resolution ^{31}P NMR spectroscopy. Such mapping could link changes in the PME region to disturbances of particular biochemical pathways, and lead to a better understanding and utilization of PME changes for diagnostic and/or treatment purposes.

^{18}O-assisted ^{31}P NMR spectroscopy was derived for NMR purposes [11,22,32–34] from the original mass spectrometry-based ^{18}O-labeling procedure [37–40,64]. Although ^{18}O-assisted high-resolution ^{31}P NMR is less sensitive than mass spectrometric analysis, it does provide advantages of simpler and quicker processing of samples and simultaneous determination of energetically-relevant, phosphoryl-containing, metabolites and their respective turnover rates [11,33,34]. In a single experiment one can measure creatine kinase, adenylate kinase and glycolytic phosphotransfer fluxes, as well as ATP production, consumption and total turnover rates, providing a comprehensive analysis of dynamic alterations in the energetic system of an intact cell [11]. Using saturation transfer ^{31}P NMR (ST ^{31}P NMR) spectroscopy, an alternative method based on monitoring magnetization transfer from gATP to CrP [15,26,31,65,66], significant CK phosphotransfer deficit was also shown during low-flow ischemia [30] or upon reperfusion following ischemia [65,67]. This is in line with results obtained in the present and previous studies with ^{18}O-assisted ^{31}P NMR spectroscopy [11,22,32]. However, in contrast to ST ^{31}P NMR spectroscopy which measures unidirectional phosphoryl exchange rates [26, 66], ^{18}O-assisted ^{31}P NMR spectroscopy detects net phosphoryl flux not only through CK but also through other phosphotransfer pathways, such as that catalyzed by AK, not readily detectable by ST ^{31}P NMR in intact heart.

Furthermore, this study shows specific benefits stemming from the combined use of high-resolution ^{31}P and ^{1}H NMR spectroscopy that accompanies ^{18}O analysis. In particular, this includes component analysis of the PME region in ^{31}P NMR spectra, determination of adenine nucleotides and their degradation products in the aromatic region of ^{1}H NMR spectra, and lactate determinations in the aliphatic region of ^{1}H NMR spectra. To study cardiac energetics in hypoxia, particular advantage was taken from the aromatic region of ^{1}H NMR spectra (5–9 ppm) where signals originating from single protons bound to carbon within nucleotide bases can be detected. Although seldom used, successful analysis of the aromatic region with high-resolution ^{1}H NMR [11,68–72], and ^{1}H-^{31}P or ^{1}H-^{13}C heteronuclear NMR [33,72] is possible. Here, we show that valuable information on tissue energetics could be obtained with high-resolution ^{1}H NMR spectroscopy both from aromatic and aliphatic region of spectra.

In conclusion, metabolic rearrangements in the intact myocardium under hypoxic stress were mapped using ^{18}O-assisted ^{31}P NMR spectroscopy, in conjunction with ^{1}H NMR. Capturing cellular energetic dynamics and associated generation of metabolic signals in hypoxia, provides further insight into mechanisms responsible for induction of stress tolerance. Thus, analysis of ^{18}O induced shifts in ^{31}P NMR spectra of cellular phosphates, the PME region of ^{31}P NMR spectra, as well as aromatic and aliphatic regions of ^{1}H NMR spectra, provides valuable information on the adjustment of cellular bioenergetics in response to challenge.

Acknowledgments

Supported by the National Institutes of Health, American Heart Association, Marriott Foundation, Miami Heart Research Institute, Bruce and Ruth Rappaport Program, and Clinician-Investigator Program at the Mayo Clinic. A.T. is an Established Investigator of the American Heart Association.

Abbreviations

AK
adenylate kinase

AMP
adenosine monophosphate

αGP
alpha-glycerophosphate

αGPDH
alpha-glycerophosphate dehydrogenase

CrP
creatine phosphate

CK
creatine kinase

GAPDH
glyceraldehyde-3-phosphate dehydrogenase

G6P
glucoso-6-phosphate

IMP
inosine monophosphate

K-H
Krebs-Henseleit

LDH
lactate dehydrogenase

MDP
methylene diphosphonate

NMP
nucleotide monophoshate

PFK
phosfofructokinase

PME
phosphomonoester

TSP
3-trimethylsilyl tetradeutero sodium propionate

References

1. Jennings RB, Reimer KA. The cell biology of acute myocardial ischemia. Annu Rev Med 1991;42:225–246. [PubMed: 2035969]
2. Saks VA, Tiivel T, Kay L, Novel-Chate V, Daneshrad Z, Rossi A, Fontaine E, Keriel C, Leverve X, Ventura-Clapier R, Anflous K, Samuel JL, Rappaport L. On the regulation of cellular energetics in health and disease. Mol Cell Biochem 1996;160–161:195–208.
3. Opie, LH. Biochemical changes associated with reversible myocardial ischemia. In: Heyndricks, GR.; Vatner, SF.; Wijns, W., editors. Clinical Pathophysiology of Myocardial Ischemia. Lippincot-Raven; New York: 1997. p. 1-19.
4. Taegtmeyer H, King LM, Jones BE. Energy substrate metabolism, myocardial ischemia, and targets for pharmacotherapy. Am J Cardiol 1998;82:54K–60K. [PubMed: 9671009]
5. Piper HM. Energy deficiency, calcium overload or oxidative stress: Possible causes of irreversible ischemic myocardial injury. Klin Wochenschr 1989;67:465–476. [PubMed: 2659881]
6. Di Lisa F. Mitochondrial contribution in the progression of cardiac ischemic injury. IUBMB Life 2001;52:255–261. [PubMed: 11798040]
7. Murry CE, Jennings RB, Reimer KA. Preconditioning with ischemia: A delay of lethal cell injury in ischemic myocardium. Circulation 1986;74:1124–1136. [PubMed: 3769170]
8. Dzeja PP, Terzic A. Phosphotransfer networks and cellular energetics. J Exp Biol 2003;206:2039–2047. [PubMed: 12756286]
9. Opie LH, Sack MN. Metabolic plasticity and the promotion of cardiac protection in ischemia and ischemic preconditioning. J Mol Cell Cardiol 2002;34:1077–1089. [PubMed: 12392880]
10. Taegtmeyer H. Genetics of energetics: Transcriptional responses in cardiac metabolism. Ann Biomed Eng 2000;28:871–876. [PubMed: 11144670]
11. Pucar D, Dzeja PP, Bast P, Juranic N, Macura S, Terzic A. Cellular energetics in the preconditioned state: Protective role for phosphotransfer reactions captured by ^{18}O-assisted ^{31}P NMR. J Biol Chem 2001;276:44812–44819. [PubMed: 11583991]
12. Barger PM, Kelly DP. PPAR signaling in the control of cardiac energy metabolism. Trends Cardiovasc Med 2000;10:238–245. [PubMed: 11282301]
13. Fryer RM, Auchampach JA, Gross GJ. Therapeutic receptor targets of ischemic preconditioning. Cardiovasc Res 2002;55:520–525. [PubMed: 12160948]
14. Bessman SP, Carpenter CL. The creatine-creatine phosphate energy shuttle. Annu Rev Biochem 1985;54:831–862. [PubMed: 3896131]
15. Bittl JA, Ingwall JS. Reaction rates of creatine kinase and ATP synthesis in the isolated rat heart. A ^{31}P NMR magnetization transfer study. J Biol Chem 1985;260:3512–3517. [PubMed: 3972835]
16. Wallimann T, Wyss M, Brdiczka D, Nicolay K, Eppenberger HM. Intracellular compartmentation, structure and function of creatine kinase isoenzymes in tissues with high and fluctuating energy demands: The 'phosphocreatine circuit' for cellular energy homeostasis. Biochem J 1992;281:21–40. [PubMed: 1731757]
17. Saks VA, Khuchua ZA, Vasilyeva EV, Belikova OY, Kuznetsov AV. Metabolic compartmentation and substrate channelling in muscle cells. Role of coupled creatine kinases in in vivo regulation of cellular respiration – a synthesis. Mol Cell Biochem 1994;133–134:155–192.
18. Dzeja PP, Zeleznikar RJ, Goldberg ND. Adenylate kinase: kinetic behavior in intact cells indicates it is integral to multiple cellular processes. Mol Cell Biochem 1998;184:169–182. [PubMed: 9746320]
19. Dzeja PP, Vitkevicius KT, Redfield MM, Burnett JC, Terzic A. Adenylate kinase-catalyzed phosphotransfer in the myocardium: Increased contribution in heart failure. Circ Res 1999;84:1137–1143. [PubMed: 10347088]
20. Ventura-Clapier R, Kuznetsov A, Veksler V, Boehm E, Anflous K. Functional coupling of creatine kinases in muscles: Species and tissue specificity. Mol Cell Biochem 1998;184:231–247. [PubMed: 9746324]
21. Dzeja PP, Redfield MM, Burnett JC, Terzic A. Failing energetics in failing hearts. Curr Cardiol Rep 2000;2:212–217. [PubMed: 10980895]

22. Pucar D, Janssen E, Dzeja PP, Juranic N, Macura S, Wieringa B, Terzic A. Compromised energetics in the adenylate kinase AK1 gene knockout heart under metabolic stress. J Biol Chem 2000;275:41424–41429. [PubMed: 11006295]
23. Janssen E, Dzeja PP, Oerlemans F, Simonetti AW, Heerschap A, de Haan A, Rush PS, Terjung RR, Wieringa B, Terzic A. Adenylate kinase 1 gene deletion disrupts muscle energetic economy despite metabolic rearrangement. EMBO J 2000;19:6371–6381. [PubMed: 11101510]
24. Gudbjarnason S, Mathes P, Ravens KG. Functional compartmentation of ATP and creatine phosphate in heart muscle. J Mol Cell Cardiol 1970;1:325–339. [PubMed: 5519941]
25. Rovetto MJ, Whitmer JT, Neely JR. Comparison of the effects of anoxia and whole heart ischemia on carbohydrate utilization in isolated working rat hearts. Circ Res 1973;32:699–711. [PubMed: 4715192]
26. Sako EY, Kingsley-Hickman PB, From AH, Foker JE, Ugurbil K. ATP synthesis kinetics and mitochondrial function in the postischemic myocardium as studied by ^{31}P NMR. J Biol Chem 1988;263:10600–10607. [PubMed: 3392029]
27. Neubauer S, Newell JB, Ingwall JS. Metabolic consequences and predictability of ventricular fibrillation in hypoxia. A ^{31}P- and ^{23}Na-nuclear magnetic resonance study of the isolated rat heart. Circulation 1992;86:302–310. [PubMed: 1617781]
28. Van Wylen DG. Effect of ischemic preconditioning on interstitial purine metabolite and lactate accumulation during myocardial ischemia. Circulation 1994;89:2283–2289. [PubMed: 8181154]
29. Ventura-Clapier R, Veksler V, Hoerter JA. Myofibrillar creatine kinase and cardiac contraction. Mol Cell Biochem 1994;133–134:125–144.
30. Hamman BL, Bittl JA, Jacobus WE, Allen PD, Spencer RS, Tian R, Ingwall JS. Inhibition of the creatine kinase reaction decreases the contractile reserve of isolated rat hearts. Am J Physiol 1995;269:H1030–H1036. [PubMed: 7573498]
31. Zhang J, Ugurbil K, From AH, Bache RJ. Use of magnetic resonance spectroscopy for *in vivo* evaluation of high-energy phosphate metabolism in normal and abnormal myocardium. J Cardiovasc Magn Reson 2000;2:23–32. [PubMed: 11545104]
32. Pucar D, Bast P, Gumina RJ, Lim L, Drahl C, Juranic N, Macura S, Janssen E, Wieringa B, Terzic A, Dzeja PP. Adenylate kinase AK1 knockout heart: Energetics and functional performance under ischemia-reperfusion. Am J Physiol 2002;283:H776–H782.
33. Dzeja PP, Pucar D, Bast P, Juranic N, Macura S, Terzic A. Captured cellular adenylate kinase-catalyzed phosphotransfer using ^{18}O-assisted ^{31} P NMR. MAGMA 2002;14:180–181.
34. Pucar D, Dzeja PP, Bast P, Juranic N, Macura S, Terzic A. ^{18}O-assisted ^{31}P NMR: A novel approach to monitor the dynamics of energy metabolism in intact heart muscle. MAGMA 2002;14:178–180.
35. Cohn M, Hu A. Isotopic ^{18}O shift in ^{31}P nuclear magnetic resonance applied to a study of enzyme-catalyzed phosphate – phosphate exchange and phosphate (oxygen) – water exchange reactions. Proc Natl Acad Sci USA 1978;75:200–203. [PubMed: 203929]
36. Hackney DD, Rosen G, Boyer PD. Subunit interaction during catalysis: Alternating site cooperativity in photophosphorylation shown by substrate modulation of [^{18}O]ATP species formation. Proc Natl Acad Sci USA 1979;76:3646–3650. [PubMed: 291029]
37. Dawis SM, Walseth TF, Deeg MA, Heyman RA, Graeff RM, Goldberg ND. Adenosine triphosphate utilization rates and metabolic pool sizes in intact cells measured by transfer of ^{18}O from water. Biophys J 1989;55:79–99. [PubMed: 2930826]
38. Zeleznikar RJ, Goldberg ND. Kinetics and compartmentation of energy metabolism in intact skeletal muscle determined from ^{18}O labeling of metabolite phosphoryls. J Biol Chem 1991;266:15110–15119. [PubMed: 1869545]
39. Dzeja PP, Zeleznikar RJ, Goldberg ND. Suppression of creatine kinase-catalyzed phosphotransfer results in increased phosphoryl transfer by adenylate kinase in intact skeletal muscle. J Biol Chem 1996;271:12847–12851. [PubMed: 8662747]
40. Zeleznikar RJ, Dzeja PP, Goldberg ND. Adenylate kinase-catalyzed phosphoryl transfer couples ATP utilization with its generation by glycolysis in intact muscle. J Biol Chem 1995;270:7311–7319. [PubMed: 7706272]
41. Laclau MN, Boudina S, Thambo JB, Tariosse L, Gouverneur G, Bonoron-Adele S, Saks VA, Garlid KD, Dos Santos P. Cardioprotection by ischemic preconditioning preserves mitochondrial function

and functional coupling between adenine nucleotide translocase and creatine kinase. J Mol Cell Cardiol 2001;33:947–956. [PubMed: 11343417]

42. Terzic A, Tung RT, Inanobe A, Katada T, Kurachi Y. G proteins activate ATP-sensitive K^+ channels by antagonizing ATP-dependent gating. Neuron 1994;12:885–893. [PubMed: 8161458]
43. Jovanovic A, Lopez JR, Alekseev AE, Shen WK, Terzic A. Adenosine prevents K^+-induced Ca^{2+} loading: Insight into cardioprotection during cardioplegia. Ann Thorac Surg 1998;65:586–591. [PubMed: 9485282]
44. Hohl CM. AMP deaminase in piglet cardiac myocytes: effect on nucleotide metabolism during ischemia. Am J Physiol 1999;276:H1502–H1510. [PubMed: 10330232]
45. Virag L, Szabo C. Purines inhibit poly(ADP-ribose) polymerase activation and modulate oxidant-induced cell death. FASEB J 2001;15:99–107. [PubMed: 11149897]
46. Camara-Artigas A, Parody-Morreale A, Baron C. Analogous activation of bovine liver glycogen phosphorylase by AMP and IMP. Int J Biochem Cell Biol 1997;29:849–856. [PubMed: 9251252]
47. Rovetto MJ, Lamberton WF, Neely JR. Mechanisms of glycolytic inhibition in ischemic rat hearts. Circ Res 1975;37:742–751. [PubMed: 157]
48. Doenst T, Han Q, Goodwin GW, Guthrie PH, Taegtmeyer H. Insulin does not change the intracellular distribution of hexokinase in rat heart. Am J Physiol 1998;275:E558–E567. [PubMed: 9755073]
49. Kubo S, Noda LH. Adenylate kinase of porcine heart. Eur J Biochem 1974;48:325–331. [PubMed: 4375035]
50. Elvir-Mairena JR, Jovanovic A, Gomez LA, Alekseev AE, Terzic A. Reversal of the ATP-liganded state of ATP-sensitive K^+ channels by adenylate kinase activity. J Biol Chem 1996;271:31903–31908. [PubMed: 8943234]
51. Dzeja PP, Terzic A. Phosphotransfer reactions in the regulation of ATP-sensitive K^+ channels. FASEB J 1998;12:523–529. [PubMed: 9576479]
52. Carrasco AJ, Dzeja PP, Alekseev AE, Pucar D, Zingman LV, Abraham MR, Hodgson D, Bienengraeber M, Puceat M, Janssen E, Wieringa B, Terzic A. Adenylate kinase phosphotransfer communicates cellular energetic signals to ATP-sensitive potassium channels. Proc Natl Acad Sci USA 2001;98:7623–7628. [PubMed: 11390963]
53. Zingman LV, Hodgson DM, Bast PH, Kane GC, Perez-Terzic C, Gumina RJ, Pucar D, Bienengraeber M, Dzeja PP, Miki T, Seino S, Alekseev AE, Terzic A. Kir6.2 is required for adaptation to stress. Proc Natl Acad Sci USA 2002;99:13278–13283. [PubMed: 12271142]
54. Suzuki M, Sasaki N, Miki T, Sakamoto N, Ohmoto-Sekine Y, Tamagawa channels M, Seino S, Marban E, Nakaya H. Role of sarcolemmal K_{ATP} in cardioprotection against ischemia/reperfusion injury in mice. J Clin Invest 2002;109:509–516. [PubMed: 11854323]
55. Gumina RJ, Pucar D, Bast P, Hodgson DM, Kurtz CE, Dzeja PP, Miki T, Seino S, Terzic A. Knockout of Kir6.2 negates ischemic preconditioning-induced protection of myocardial energetics. Am J Physiol 2003;284:H2106–H2113.
56. Hardie DG. Roles of the AMP-activated/SNF1 protein kinase family in the response to cellular stress. Biochem Soc Symp 1999;64:13–27. [PubMed: 10207618]
57. Blair E, Redwood C, Ashrafian H, Oliveira M, Broxholme J, Kerr B, Salmon A, Ostman-Smith I, Watkins H. Mutations in the gamma(2) subunit of AMP-activated protein kinase cause familial hypertrophic cardiomyopathy: Evidence for the central role of energy compromise in disease pathogenesis. Hum Mol Genet 2001;10:1215–1220. [PubMed: 11371514]
58. Ottaway JH, Mowbray J. The role of compartmentation in the control of glycolysis. Curr Top Cell Reg 1977;12:107–208.
59. Jeffrey FM, Storey CJ, Malloy CR. Predicting functional recovery from ischemia in the rat myocardium. Basic Res Cardiol 1992;87:548–558. [PubMed: 1485887]
60. Auffermann W, Wagner S, Wu S, Buser P, Parmley WW, Wikman-Coffelt J. Calcium inhibition of glycolysis contributes to ischaemic injury. Cardiovasc Res 1990;24:510–520. [PubMed: 2143696]
61. Van Dobbenburgh JO, Lahpor JR, Woolley SR, de Jonge N, Klopping C, Van Echteld CJ. Functional recovery after human heart transplantation is related to the metabolic condition of the hypothermic donor heart. Circulation 1996;94:2831–2836. [PubMed: 8941109]

62. Schaefer S, Carr LJ, Prussel E, Ramasamy R. Effects of glycogen depletion on ischemic injury in isolated rat hearts: Insights into preconditioning. Am J Physiol 1995;268:H935–H944. [PubMed: 7900892]
63. Auffermann W, Wu ST, Parmley WW, Wikman-Coffelt J. Glycolysis in heart failure: A ^{31}P-NMR and surface fluorometry study. Basic Res Cardiol 1990;85:342–357. [PubMed: 2241766]
64. Zeleznikar RJ, Heyman RA, Graeff RM, Walseth TF, Dawis SM, Butz EA, Goldberg ND. Evidence for compartmentalized adenylate kinase catalysis serving a high energy phosphoryl transfer function in rat skeletal muscle. J Biol Chem 1990;265:300–311. [PubMed: 2152922]
65. Neubauer S, Hamman BL, Perry SB, Bittl JA, Ingwall JS. Velocity of the creatine kinase reaction decreases in postischemic myocardium: A ^{31}P-NMR magnetization transfer study of the isolated ferret heart. Circ Res 1988;63:1–15. [PubMed: 3383370]
66. Joubert F, Gillet B, Mazet JL, Mateo P, Beloeil J, Hoerter JA. Evidence for myocardial ATP compartmentation from NMR inversion transfer analysis of creatine kinase fluxes. Biophys J 2000;79:1–13. [PubMed: 10866933]
67. Hugel S, Horn M, de Groot M, Remkes H, Dienesch C, Hu K, Ertl G, Neubauer S. Effects of ACE inhibition and beta-receptor blockade on energy metabolism in rats postmyocardial infarction. Am J Physiol 1999;277:H2167–H2175. [PubMed: 10600834]
68. van Zijl PC, Moonen CT. *In situ* changes in purine nucleotide and N-acetyl concentrations upon inducing global ischemia in cat brain. Magn Reson Med 1993;29:381–385. [PubMed: 8095689]
69. Middleton DA, Hockings PD, Glen S, Reid DG, Rose SE, Crozier S, Roffman W, Rothaul AL, Hunter AJ, Doddrell DM. Image directed proton spectroscopy of gerbil brain at 7 tesla. NMR Biomed 1995;8:118–126. [PubMed: 8579999]
70. Decanniere C, Eleff S, Davis D, van Zijl PC. Correlation of rapid changes in the average water diffusion constant and the concentrations of lactate and ATP breakdown products during global ischemia in cat brain. Magn Reson Med 1995;34:343–352. [PubMed: 7500873]
71. Stromski ME, Cooper K, Thulin G, Gaudio KM, Siegel NJ, Shulman RG. Chemical and functional correlates of postischemic renal ATP levels. Proc Natl Acad Sci USA 1986;83:6142–6145. [PubMed: 3461481]
72. Pollesello P, Eriksson O, Vittur F, Paoletti S, Geimonen E, Toffanin R. Detection and quantitation of phosphorus metabolites in crude tissue extracts by ^{1}H and ^{31}P NMR: Use of gradient assisted ^{1}H-^{31}P HMQC experiments, with selective pulses, for the assignment of less abundant metabolites. NMR Biomed 1995;8:190–196. [PubMed: 8664104]
73. Kalic M, Busselmann G, Lauterwein J, Kamp G. Phosphorous metabolites in boar spermatozoa. Identification of AMP by multinuclear magnetic resonance. Biochim Biophys Acta 1997;1320:208–216. [PubMed: 9210287]

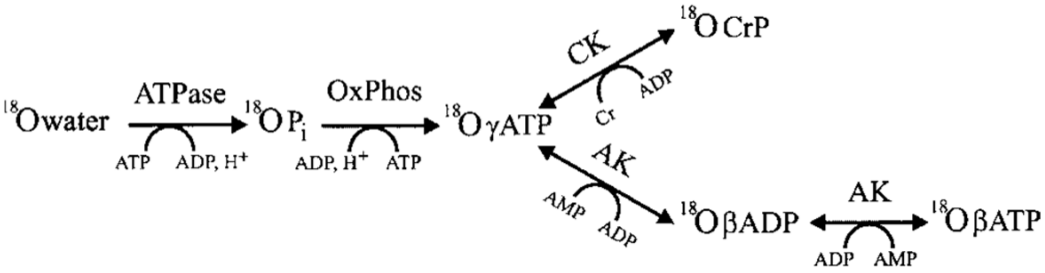

Fig. 1.

Sequences in labeling of cellular phosphates by ^{18}O. On perfusion of isolated hearts with media enriched in ^{18}O water, ^{18}O first incorporates into inorganic phosphate (P_i) by cellular ATPases. Then, ATP synthesis by oxidative phosphorylation and glycolysis introduce ^{18} O-labeled P_i into -phosphate of ATP. Creatine kinase transfers ^{18}O-labeled phosphoryl from -ATP to CrP, while adenylate kinase transfers ^{18}O-labeled phosphoryl to βADP and βATP. In this way, the ^{18}O-phosphoryl labeling procedure detects only newly generated molecules containing ^{18}O-labeled phosphoryls reflecting cellular ATP turnover and net fluxes through individual phosphotransfer pathways.

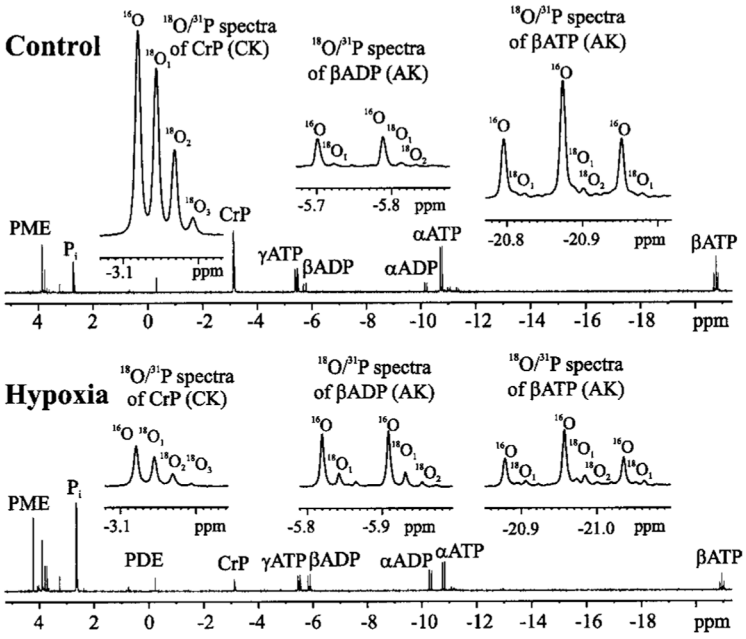

Fig. 2.

Reduced creatine kinase and increased adenylate kinase phosphotransfer under hypoxia. ^{31}P NMR spectra, from 5 to −21 ppm, are presented in control and hypoxic hearts. Regions of spectra that correspond to CrP, βADP and βATP peaks are magnified to illustrate the ^{18}O-induced shift following incorporation of ^{18}O atoms. Under hypoxia, ^{18}O incorporation into CrP, a consequence of creatine kinase phosphotransfer, was reduced, while ^{18}O incorporation into βADP and βATP resulting from adenylate kinase phosphotransfer was increased. Incorporation of each ^{18}O atom induces an isotope shift of 0.0250 in ^{31}P NMR spectra of CrP and 0.0228 ppm in βADP, respectively. The isotope shift of βATP was different for bridging and non-bridging ^{18}O oxygens, 0.0170 and 0.0287 ppm, respectively. ^{16}O, $^{18}O_1$, $^{18}O_2$and $^{18}O_3$ indicate species of phosphoryls containing 0, 1, 2 and 3 of atoms of ^{18}O. Up to three ^{18}O atoms, can be incorporated in phosphoryls of CrP, βADP and βATP. Peaks corresponding to bridging and non-bridging ^{18}O oxygens of βATP are marked as one peak. PME – phosphomonoester region; Pi – inorganic phosphate; PDE – phosphodiester region.

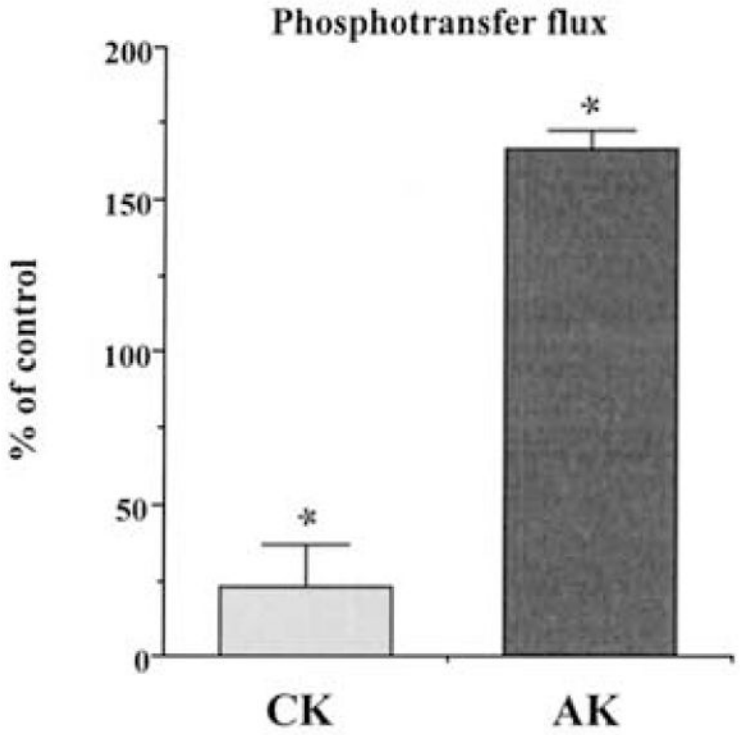

Fig. 3.

Redistribution of phosphotransfer flux between creatine kinase and adenylate kinase under hypoxic stress. Average phosphotransfer fluxes were determined from ^{18}O-labeled phosphoryl appearance in CrP, βADP and βATP, respectively. *Indicates statistically significant differences at $p < 0.01$.

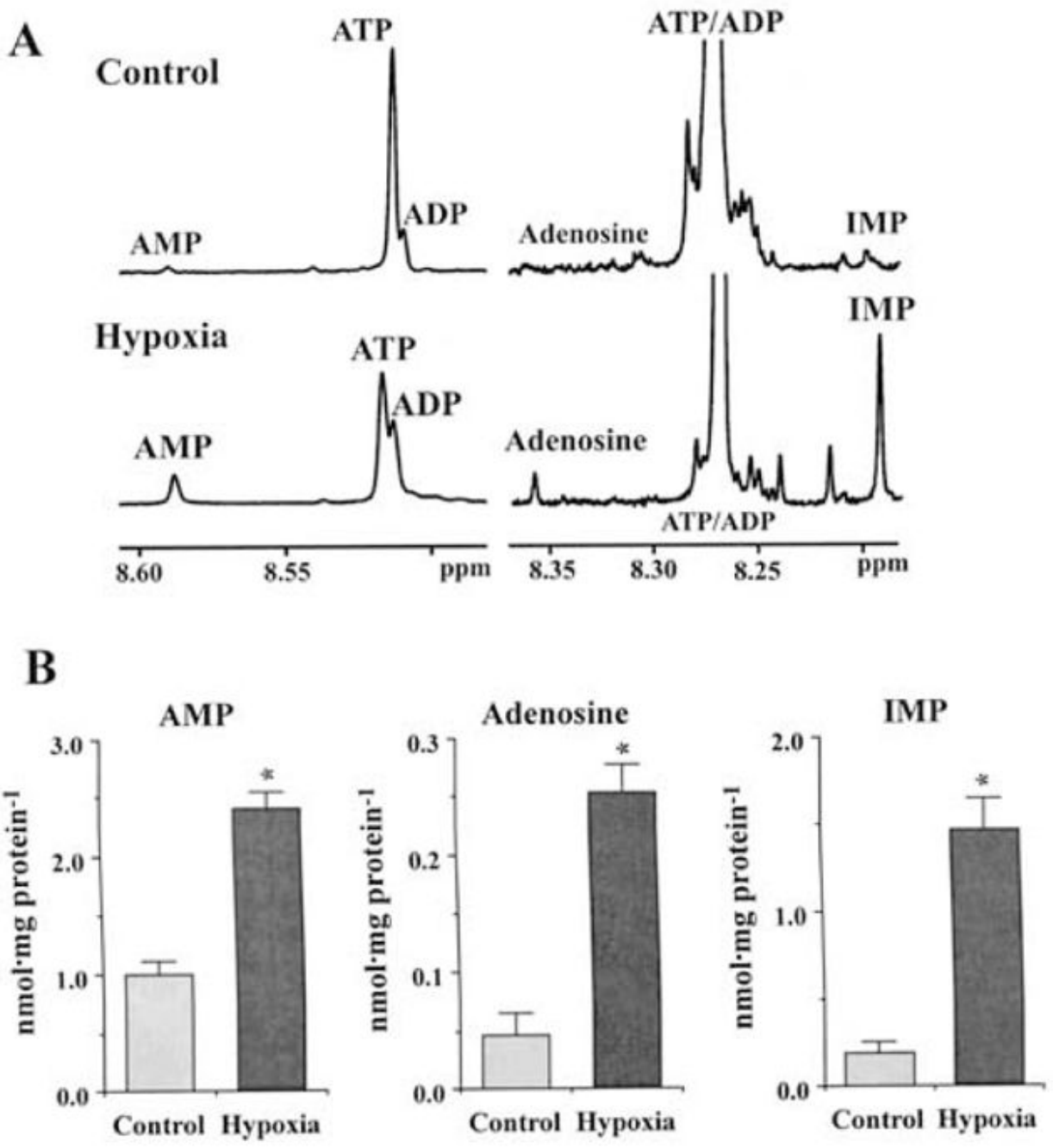

Fig. 4.

^{1}H NMR-based analysis of metabolic signals following activation of adenylate kinase phosphotransfer in hypoxia. (A) Aromatic portions (ppm 8.62–8.45 and 8.37–8.18) of ^{1}H NMR spectra with decrease of ATP and increase of ADP, AMP, adenosine and IMP in hypoxia. (B) Average metabolite levels determined from ^{1}H NMR spectra. *Indicates statistically significant differences at $p < 0.01$.

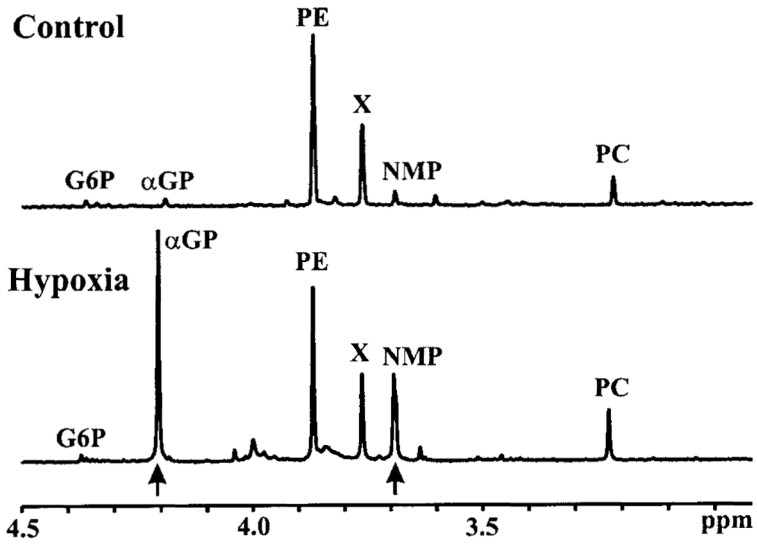

Fig. 5.

α-Glycerophosphate is a principal component of the phosphomono-ester region in ^{31}P NMR spectra under hypoxia. Phosphomonoester (PME) regions of ^{31}P NMR spectra in control and hypoxic hearts. Arrows indicate increase of α-glycerophosphate (αGP) and nucleotide monophosphates (NMP) in hypoxia. G6P – Glucoso-6-phosphate; PE – phoshoethanolamine; X – unknown resonance; PC – phosphocholine.

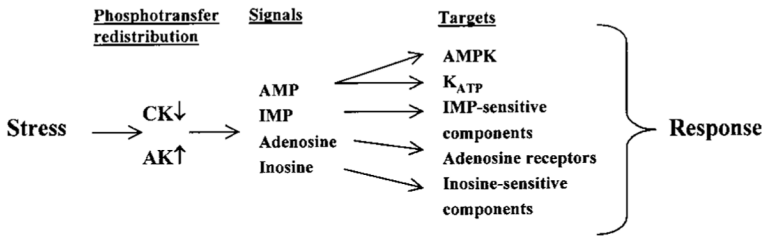

Fig. 6.

Metabolic signaling events triggered by stress-induced phosphotransfer redistribution between creatine kinase and adenylate kinase. In hypoxia, decrease in CK flux activates AK-phosphotransfer with generation of metabolic signals in the form of AMP, IMP, adenosine and inosine. These metabolites adjust the activities of ATP/ADP-, AMP-, IMP-, adenosine- and inosine-sensitive cellular components, including glycolysis/glycogenolysis, and contribute to the generation of a stress-tolerant state. AMPK – AMP-activated protein kinase; K_{ATP} – ATP-sensitive K^+ channel.